Supporting Information

Selectively Etching-off Highly Reactive (002) Zn Facet Enable Highly Efficient Aqueous Zinc-metal Batteries

Dongming Xu,[a] *Benqiang Chen,*[a] *Xueting Ren,*[a] *Chao Han,*[a] *Zhi Chang,**[a] *Anqiang Pan**[a,c], *Haoshen Zhou**[b]

[a]Department of Materials Physics and Chemistry, School of Materials Science and Engineering, Key Laboratory of Electronic Packaging and Advanced Functional Materials of Hunan Province, Central South University, Changsha, 410083, Hunan, China.

[b]Center of Energy Storage Materials & Technology, College of Engineering and Applied Sciences, Jiangsu Key Laboratory of Artificial Functional Materials, National Laboratory of Solid State Micro-structures, and Collaborative Innovation Center of Advanced Micro-structures, Nanjing University, Nanjing, 210093, P. R. China.

[c]School of Physical Science and Technology, Xinjiang University, Urumqi, Xinjiang830046, China.

E-mail: zhichang@csu.edu.cn (Prof. Z. C.), pananqiang@csu.edu.cn (Prof. A. P.), hszhou@nju.edu.cn (Prof. H. Z.).

1. Experimental Section

Zirconium chloride ($ZrCl_4$, 99.9%), p-Phthalic acid ($C_8H_6O_4$), Vanadium pentoxide (V_2O_5, 99.5%), Aniline ($C_6H_5NH_2$, 99%), Ammonium metavanadate (NH_4VO_3, 99.5%) were purchased from Aladdin reagent Co., Ltd. Zinc sulfate heptahydrate ($ZnSO_4 \cdot 7H_2O$, 99.5%), Oxalic acid ($C_2H_2O_4$, 98%) and N, N-dimethylformamide (C_3H_7NO, DMF) were purchased from Sinopharm Chemical Reagents Co., Ltd. All synthesis experiments were conducted in room temperature environment.

Material Preparation

Preparation of etched Zinc Foil. Three types of zinc foils with different crystal planes exposed were selected as the object of etching reaction. zirconium chloride (1 mmol) and terephthalic acid (2 mmol) were dissolved in DMF (50 mL), ultrasonic for 20 min to obtain a transparent solution. zinc foil (4 cm x 5 cm) was immersed into the solution for 1 hour, 2 hours, 3 hours, and 10 hours at 15 ^oC. Take out the zinc foil and wash it with water and ethanol for several times. After being soaked in ethanol for one day, the zinc foil was taken out to an oven at 80 ^oC for 5 h to obtain etched Zn foil. The zinc foil obtained by BDC or $ZrCl_4$ reaction alone is obtained without adding zirconium chloride or terephthalic acid to the precursor solution.

Electrolyte preparation. Zinc sulfate heptahydrate ($ZnSO_4 \cdot 7H_2O$) was dissolved into the deionized water to obtain the 2 M $ZnSO_4$ electrolyte.

Synthesis of PANI-V_2O_5 (PVO) cathode. V_2O_5 powder (2 mmol) was dissolved in deionized water (30 mL) at room temperature. Drop concentrated HCl into the above solution under continuous magnetic stirring to adjust the pH value of the solution to 1-2. Then, Aniline (200 μL) was added to the above mixture until a dark brown solution is obtained. Transfer the above solution to an autoclave (50 mL) and heat at 180 ^oC for 24 hours. When cool to room temperature, the dark products were washed several times with deionized water and ethanol. Finally, the above samples were dried in an oven at 60 °C for 12 hours to obtain PVO.

Preparation of $NH_4V_4O_{10}$ (NVO) cathode. NVO was synthesized by the hydrothermal method. In detail, NH_4VO_3 (2.74 mmol) was added to water (40 mL) and stirred continuously for 1 h at 60 ^oC. $H_2C_2O_4 \cdot 2H_2O$ (4.6 mmol) was dissolved to the solution and stirred for 30 min until the solution turned light blue. The mixed solution was transferred to a 100 mL reactor and placed it in an oven at 180 ^oC for 6 hours. After the black-green precipitate had been reduced

to room temperature, washed it three times with water and ethanol. The sample was dried in a vacuum oven at 60 ^{o}C for 12 hours.

2. Material characterization

TESCAN MIRA3 LMH scanning electron microscope (SEM) was used to obtain the surface morphology and cross-section. The cycled batteries were disassembled and the Zn electrodes were taken out. The Zn anodes were rinsed by deionized water for several times to wash electrolyte salt and attached glass fiber, and then transfer the electrodes to the drying oven for 20 min. Then the electrodes were transferred to a drying oven to remove the solvent. The dried Zn metal electrodes was transferred to the SEM sample chamber for observation. The X-ray diffraction data were obtained using a German Bruker D8 Advance X-ray diffractometer. The contact angle measurements were tested by a contact angle goniometer (Lauda Scientific LSA100), and the amount of electrolyte is 5 μL. The morphology of Zn dendrite growth in the electrolyte was observed using an in-situ optical microscope with a homemade symmetric cell test machine. The three-dimensional morphology and structure of the zinc surface after being cycled were tested and obtained using the KEYENCE VK-X150 confocal microscope, and the in-situ X-ray photoelectron spectroscopy was obtained using Thermo Scientific K-Alpha equipment. Electron backscattering diffraction (EBSD, Oxford insturments Nordly max3) was used to visualize the crystallographic orientation/crystal surface texture of pure bare Zn and etched Zn surfaces after cycling. TOF-SIMS analysis was completed by a TESCAN LYRA3 GM scanning electron microscope equipped with TOF-SIM accessories, and the measuring beam was 1 nA.

3. Electrochemical measurement.

To prepare PVO and NVO electrodes, the prepared PVO/NVO, super P, and PVDF were mixed and ground in a 7:2:1 mass ratio. Add the appropriate amount of NMP and thoroughly mix the mixture. The slurry obtained was coated on the stainless-steel mesh and dried at 80 ^{o}C for 12 hours. The mass load of the electrode was managed at 2 mg cm^{-2}. The high mass load of the electrode was controlled at 6-9 mg cm^{-2}. Then assemble the CR2032 coin cell for the electrochemical test. The cathode of the pouch cell is to apply the mixed slurry on the stainless steels mesh with the size of 2 cm x 3 cm /3 cm x 4 cm and control the area load at 6-7 mg cm^{-2}. Zn foil and etched Zn foil were cut into disc electrodes with a diameter of 10 mm. Glass fiber membrane (GF/D, Whatman) was used as the separator, and 2 M $ZnSO_4$ in water was used as

the electrolyte of symmetrical batteries and full cells. Noting that the amount of electrolyte for coin cells was 70 μL, and the volume of 2 M $ZnSO_4$ for pouch cell was 500 μL. Neware battery test system (CT 4008Tn 5V50mA-164) was used to test the long-term cycle, rate performance, coulomb efficiency of coin type battery and long-term cycle performance and rate performance of pouch cell with a potential range of 0.3-1.4 V at room temperature. Cyclic voltammetry (CV), electrochemical impedance spectroscopy (EIS) and linear sweep voltammetry (LSV) measurements were measured with the electrochemical workstation (CHI660). In the three-electrode measuring system, the bare zinc anode or etched zinc anode is used as the working electrode, the platinum sheet is used as the counter electrode, and the Ag/AgCl electrode protected in saturated KCl aqueous solution is used as the reference electrode for Tafel test.

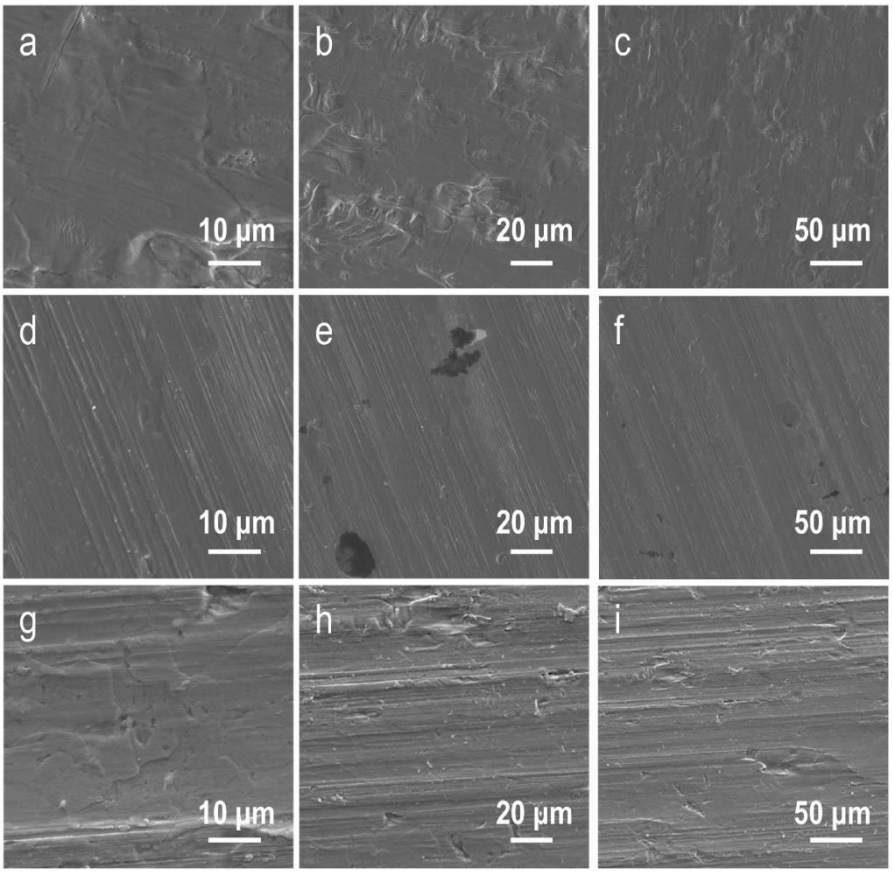

Fig. S1. The SEM images of zinc metal with different initial states and crystal planes. (a, b, c) (101)-Zn, (d, e, f) (101+002)-Zn, (g, h, i) (002)-Zn.

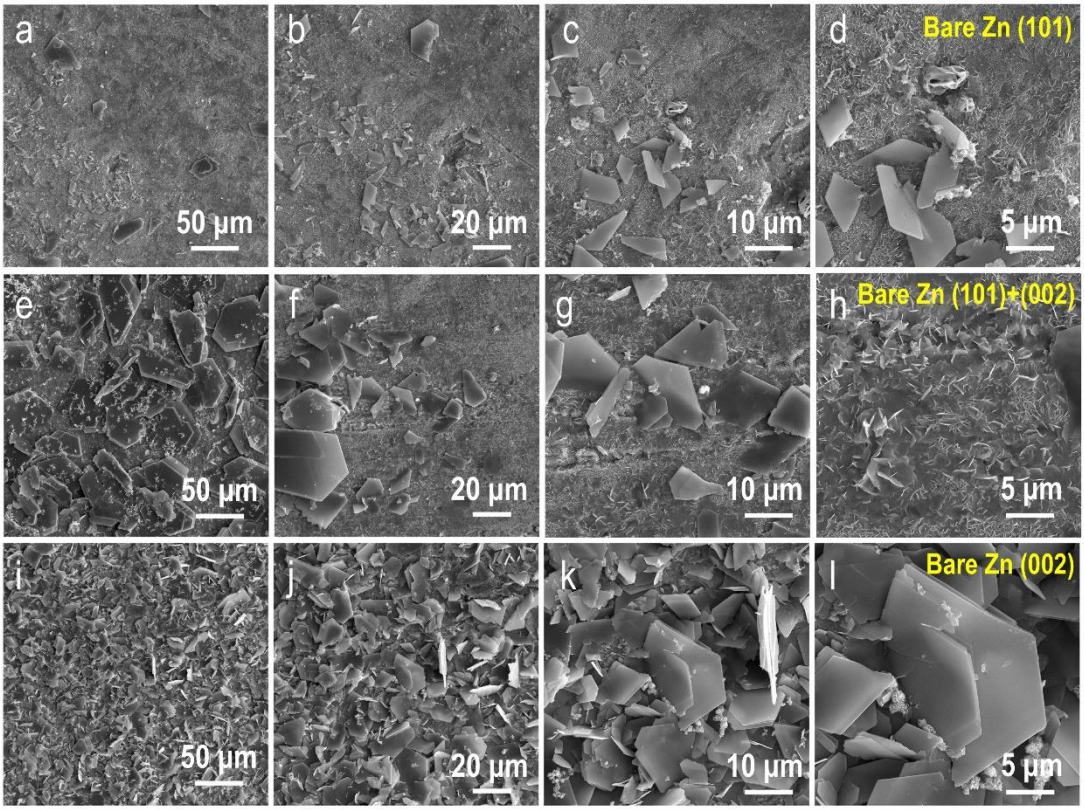

Fig. S2. SEM images of (a-d) (101)-Zn, (d-g) (101+002)-Zn, (i-l) (002)-Zn after being soaked in 2 M $ZnSO_4$-H_2O for 5 days.

In terms of a chemical reaction, zinc foils with different crystal planes react at variable speeds in the electrolyte. In the 2 M $ZnSO_4$-H_2O, the Zn (002) crystal plane is more unstable, making it simpler to produce side reactions and a significant amount of ZHS, which passivates the zinc metal surface and enhances its irreversibility. In terms of chemical reaction, the rate of side reaction of zinc foils with different crystal planes in the electrolyte is different. The zinc with (002) crystal plane is more unstable in the zinc sulfate solution, which leads to more easy side reaction and a large amount of ZHS, which makes the zinc cathode passive and promotes its irreversibility.

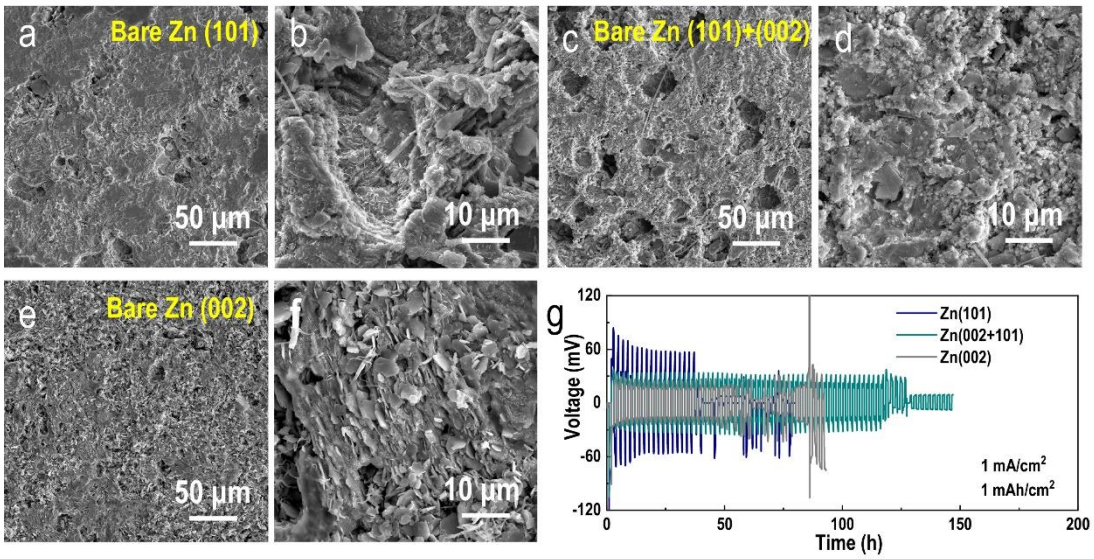

Fig. S3. SEM images of (a, b) (101)-Zn, (c, d) (101+002)-Zn, (e, f) (002)-Zn and (g) their overpotential evolution after being immersed in 2M $ZnSO_4$-H_2O electrolyte for 5 days and circulated for 50 hours in symmetrical cells.

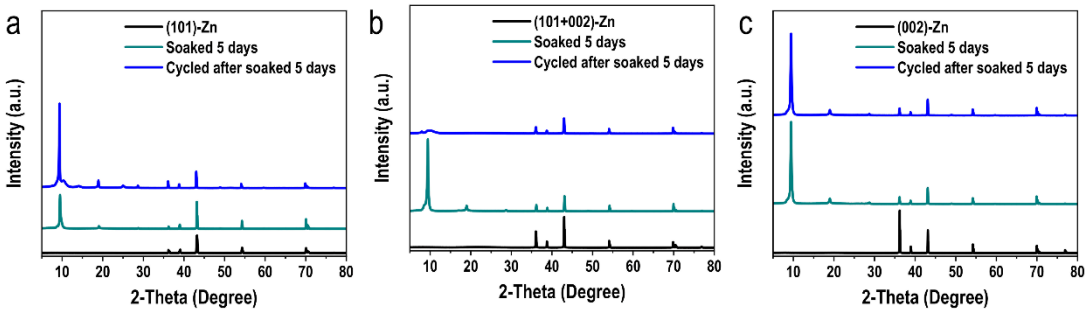

Fig. S4. The XRD of (a) (101)-Zn, (b) (101+002)-Zn, (c) (002)-Zn after being soaked and cycled for 100 hours.

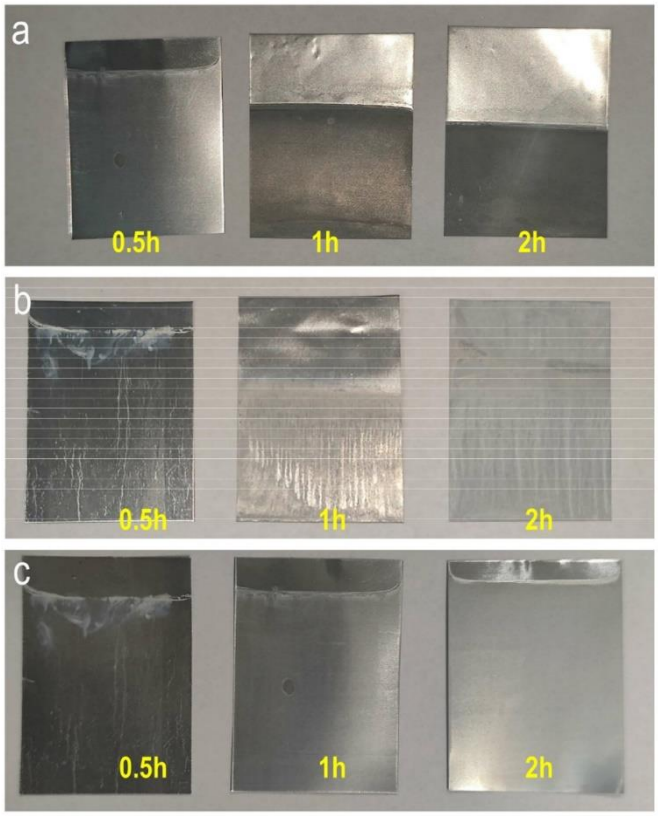

Fig. S5. Digital Photos of Zn after being immersed in the DMF solution contained (a) $ZrCl_4$, (b) BDC and (c) the combination of BDC and $ZrCl_4$.

With the prolongation of immersion time in pure $ZrCl_4$ solution, the surface of zinc foil gradually turned blacken, indicating that the microcracks on the surface of zinc were intensified. After soaking in pure BDC solution, white Zn-BDC ZIFs were produced on the surface of zinc foil. The surface of zinc foil soaked in mixed solution changes from bright to fuzzy and rough, indicating the micro-etching process of zinc surface.

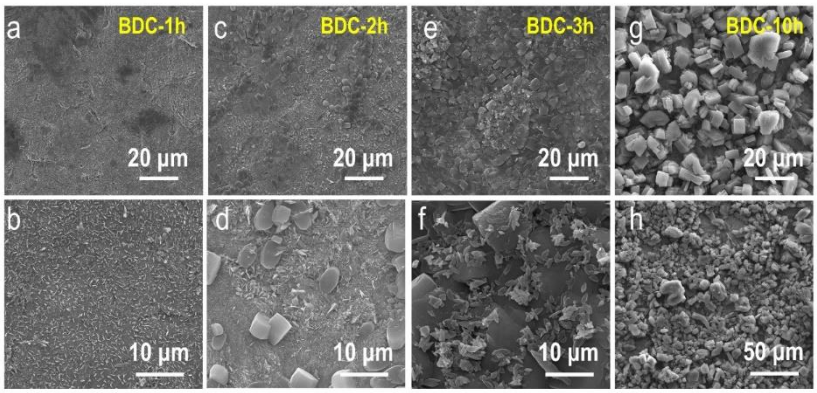

Fig. S6. SEM images of zinc foil soaked in DMF solution containing BDC for (a, b) 1 hour, (c, d) 2 hours, (e, f) 3 hours and (g, h) 10 hours.

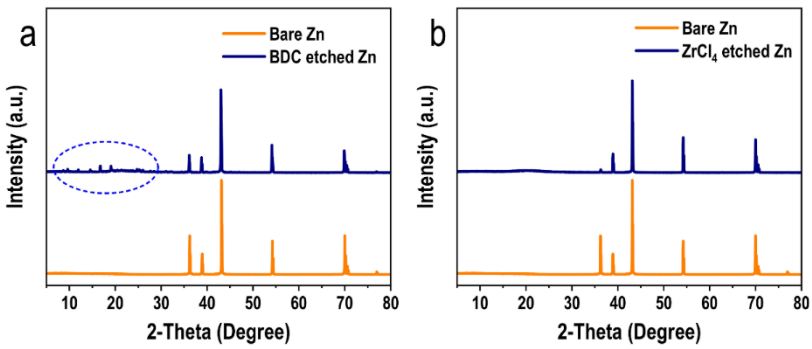

Fig. S7. XRD of zinc foil after being immersed in DMF solution containing (a) BDC or (b) $ZrCl_4$ for 2 hours.

After being soaked in DMF solution of BDC, the Zn foil showed the ZIF characteristic peak in the XRD data, and the peak of Zn (002) crystal plane reduced but was not particularly noticeable. After being soaked in DMF solution of $ZrCl_4$, The XRD data of Zn foil demonstrated that there was no by-product production, but that zirconium chloride had a selective etching impact on zinc due to a dramatic drop in the intensity of Zn (002) peak (**Fig.** S7b).

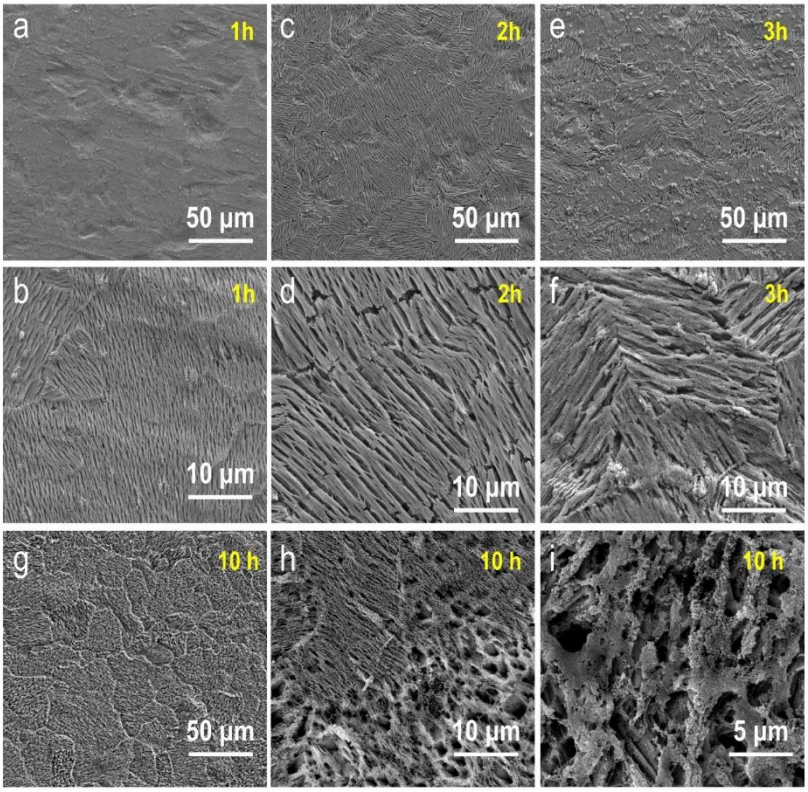

Fig. S8. SEM images of zinc foil soaked in $ZrCl_4$ solution for (a, b) 1 hour, (c, d) 2 hours, (e, f) 3 hours, (g, h, i) 10 hours.

When zinc foil was soaked in DMF solution of pure $ZrCl_4$, the zinc surface had visible flaws in the microstructure, and low magnification SEM revealed the pattern of selective etching. The cracks got bigger and more noticeable as the etching reaction time increased, and eventually corrosion pits started to show up.

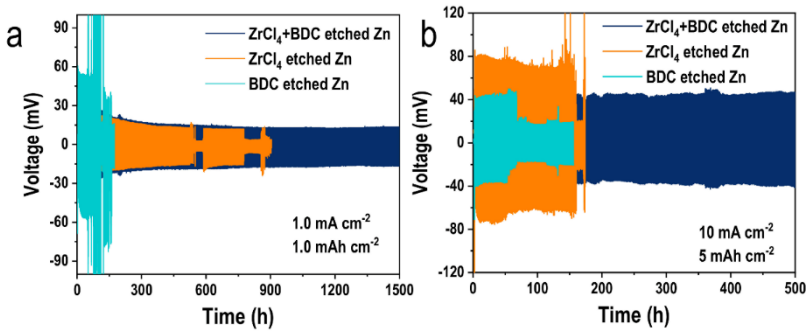

Fig. S9. Electrochemical performance of Zn/Zn symmetrical battery of Zn metal obtained under various etching conditions (single BDC, single $ZrCl_4$ or combination of BDC and $ZrCl_4$).

Zn foil immersed into the dimethylformamide (DMF) solution contained terephthalic acid (BDC) and zirconium chloride ($ZrCl_4$) as metal anodes were evaluated on symmetrical cells. Compared with the single etchant, the Zn selectively etched by mixed solution can be stably cycled for 1500 hours under a low current density of 1 mA cm^{-2} and capacity of 1 mAh cm^{-2}. The Zn (101) pillar structure created by combined etchants has a more pronounced enhancing effect on the improvement of zinc dissolution/stripping life.

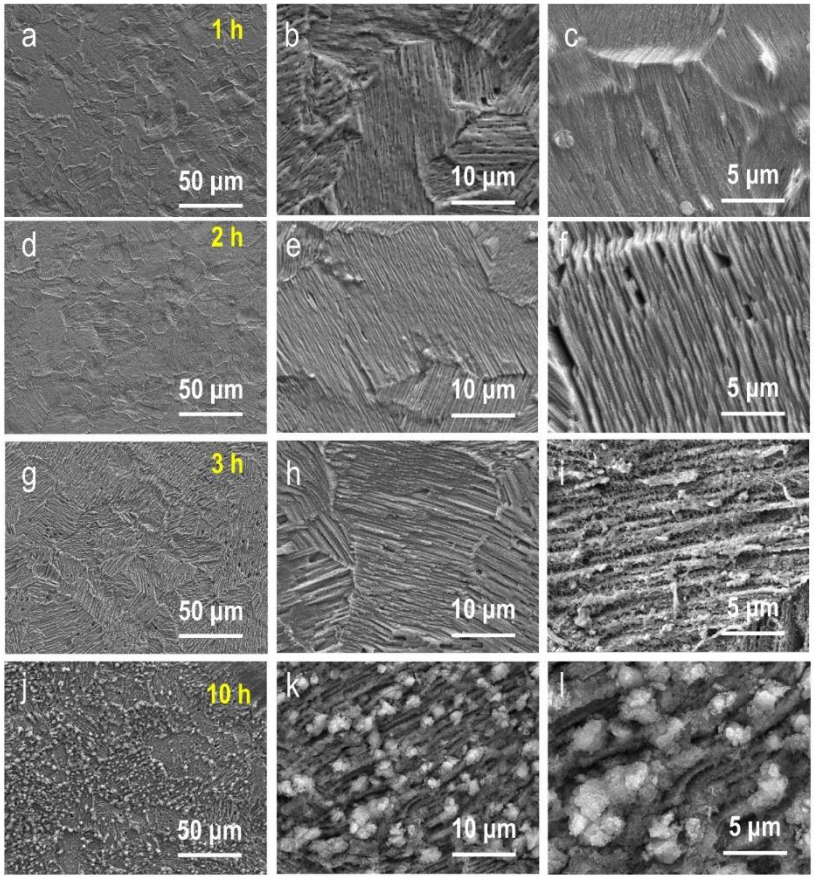

Fig. S10. SEM images of (101) Zn metal etched for (a, b, c) 1 hour, (d, e, f) 2 hours, (g, h, i) 3 hours and (j, k, l) 10 hours in the mixed solution of appropriate concentration.

We found when zinc foil was selectively etched with a solution of zirconium chloride and BDC, the size of the cracks on the zinc surface could be reduced, the reaction rate of the zinc was slowed, and the selective reaction was more thorough. The Zn surface following selective etching revealed a densely patterned lamellar structure with a thickness of roughly 300 nm after 1h of reaction. After three hours, the zinc foil's surface started to develop pits and fissures. There are lumps on the surface of the zinc foil after 10 hours of reaction, which should be the Zr-MOF produced after a lengthy reaction.

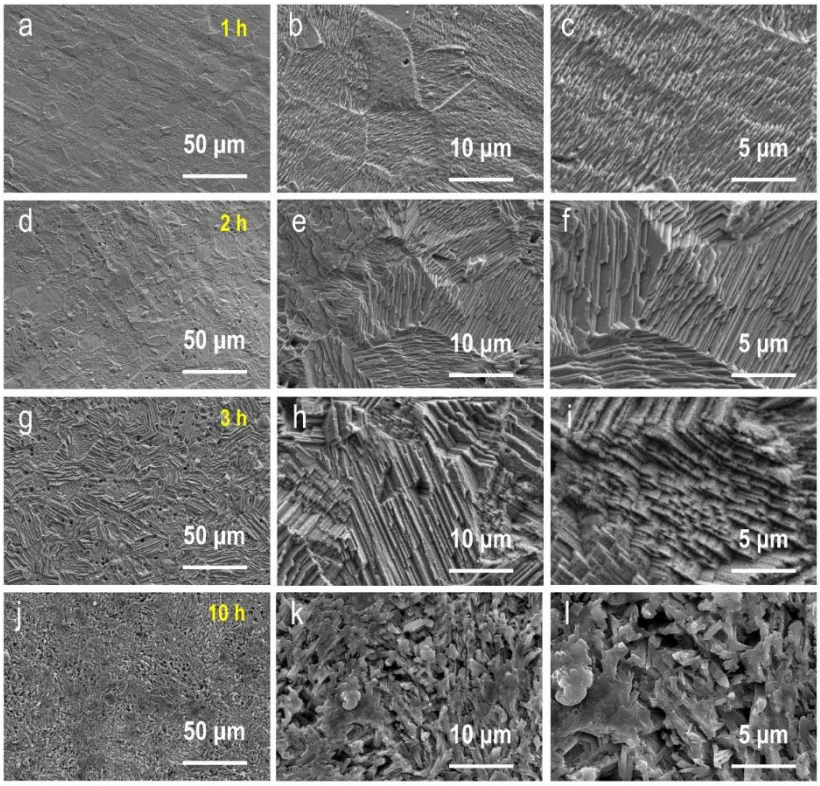

Fig. S11. SEM images of (002) Zn metal etched for (a, b, c) 1 hour, (d, e, f) 2 hours, (g, h, i) 3 hours and (j, k, l) 10 hours in the mixed solution of appropriate concentration.

After being etched, the surface structure of zinc foil with the (002) primary crystal plane differs little from zinc foil with other crystal planes.

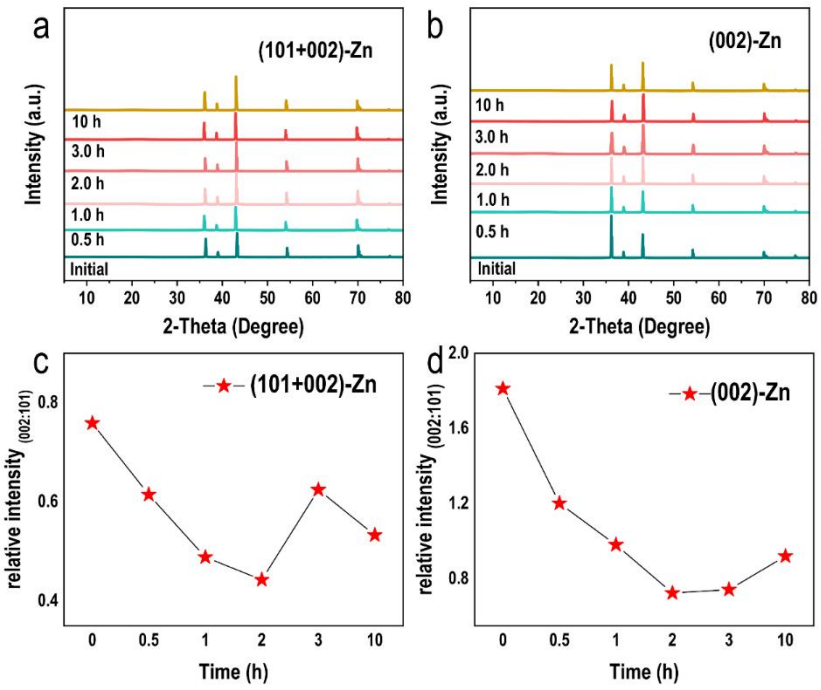

Fig. S12. XRD patterns and (002)/(101) ratio of zinc with different initial states and crystal planes after treatment in mixed solution. (a, b) XRD pattern of (101+002)-Zn and (002)-Zn soaked for 0-10 h, (c, d) the (002)/(101) peak ratio value of (101+002)-Zn and (002)-Zn after treatment in mixed solution.

The (002) crystal planes of three different types of zinc foils could be weaken under these circumstances, and after two hours of reaction, and (002) Zn achieves its lowest value.

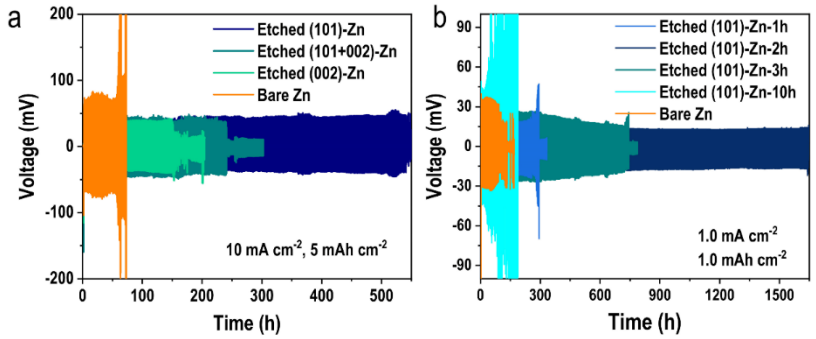

Fig. S13. (a) Electrochemical performances of Zn//Zn cells based on different Zn metals after same etching time. (b) Cyclic performance of zinc symmetrical cell based on etched Zn with different etching time.

At various reaction periods, we examined the zinc ion deposition/stripping capabilities of zinc foil. While zinc foils with different crystal planes are used as zinc cathode after etching, the lower the strength of Zn (002) peak, the better the performance of zinc under large current density and high area capacity tests, and the longer the time for stable deposition/stripping. The bare zinc will be short-circuited after only 40 hours of cycling under the conditions of 10 mA cm^{-2} and 5 mAh cm^{-2}, while the deposition/stripping performance of zinc foil with selective reduction of Zn (002) has been improved. The symmetrical battery with super high proportion of (101) Zn crystal planes can be stably cycled for more than 550h under this condition. This may be because zinc ions tend to deposit on the Zn (101) crystal plane under large current density, while the high proportion of the Zn (101) crystal plane provides this convenient condition for rapid and uniform plating/stripping.

The (101)-Zn were used as the anode for test. After one hour of etching, a short circuit happens when the stable cycle time is raised to 300 hours. The zinc ion can be constantly deposited and dissolved on zinc metal anode for 1600 hours after two hours of etching. It was possible to achieve 700 hours of temperature deposition and dissolution while using zinc foil that has been etched for three hours as the cathode. The deposition solubility of Zn-ions on etched Zn has improved somewhat when compared to the zinc foil that hasn't been treated.

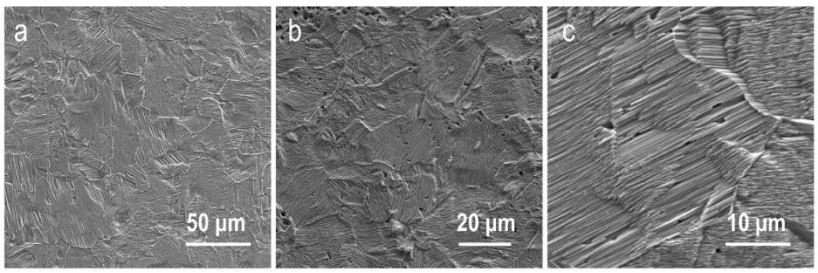

Fig. S14. SEM images of (101)-Zn after etching for 2 hours. The SEM of the Zn etching showed that a large range of vertical zinc flakes arranged in parallel appeared on the zinc surface.

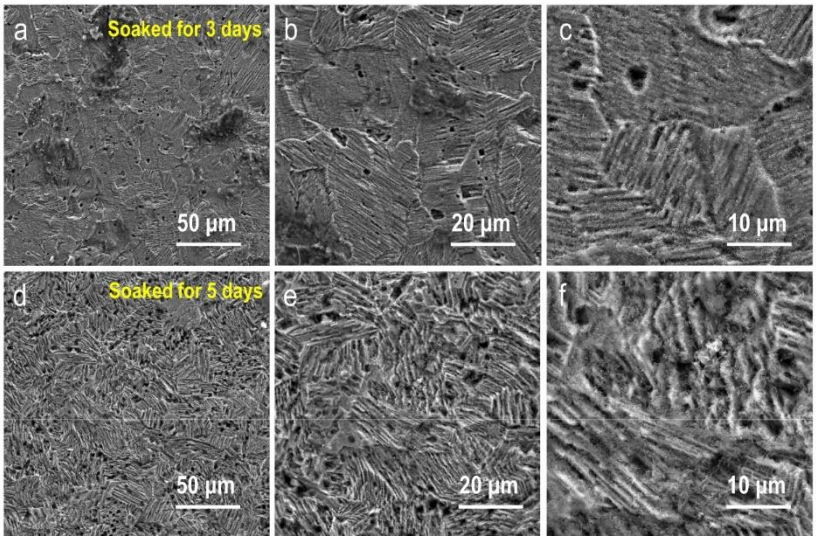

Fig. S15. SEM images of (101)-Zn soaked in 2 M $ZnSO_4$-H_2O for 3-5 days.

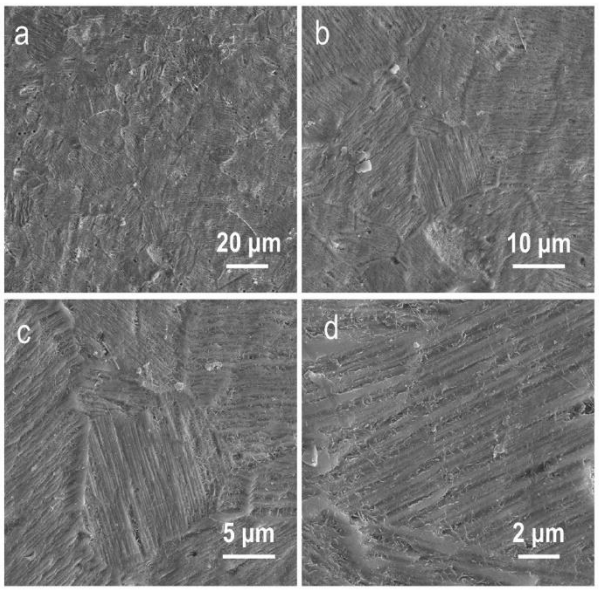

Fig. S16. SEM images of etched Zn collected from symmetrical cells after soaking for 5 days and cycling for 100 hours.

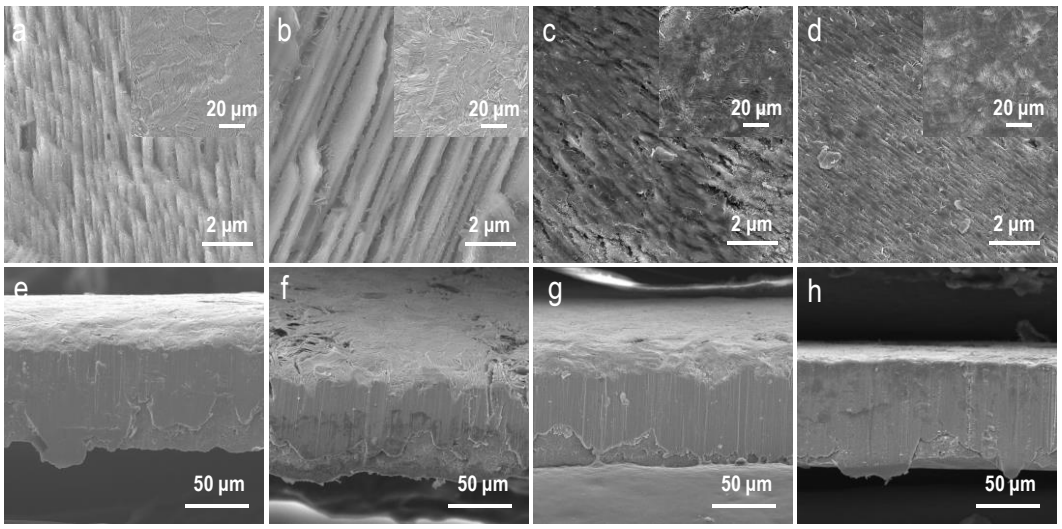

Fig. S17. (a-d) The SEM images of etched Zn electrode with Zn deposition of 1 mAh cm^{-2}, 3 mAh cm^{-2}, 5 mAh cm^{-2} and 10 mAh cm^{-2} and (e-h) the corresponding cross-section images.

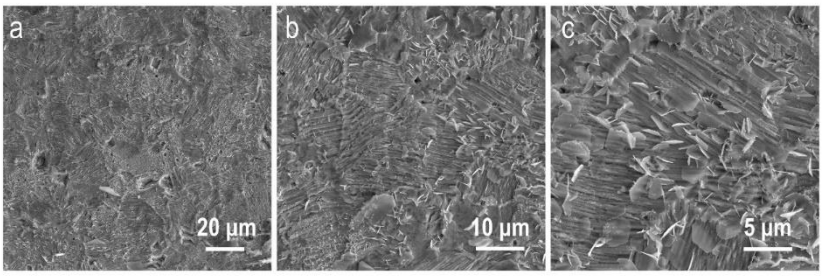

Fig. S18. SEM images of (002)-Zn soaked in 2 M $ZnSO_4$-H_2O for 5 days.

After selective etching in mixed solution, the chemical reactions, and by-products of zinc foils with different crystal faces in zinc sulfate are reduced. After being etched, zinc with high content of Zn (002) will also generate some flake ZHS due to a small amount of (002) crystal plane exposed on the surface.

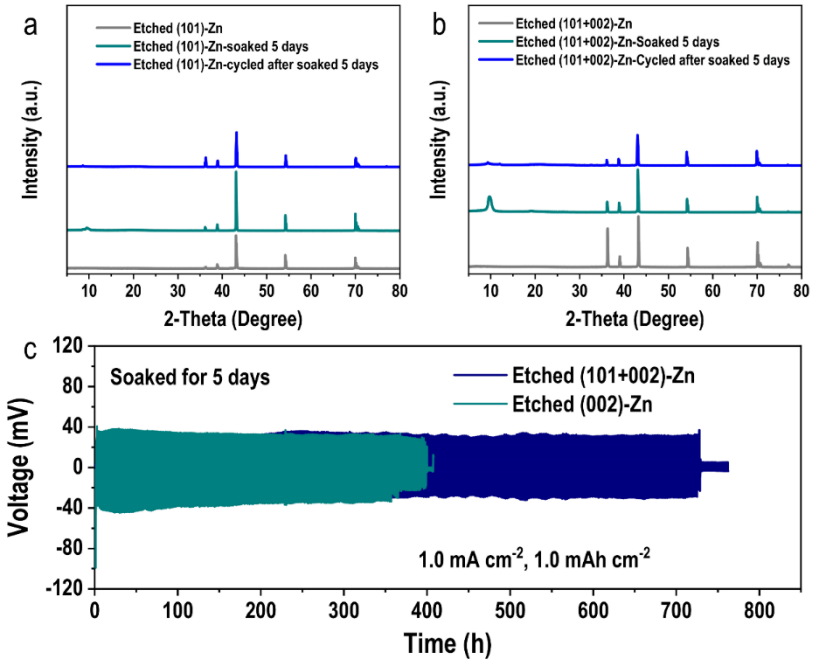

Fig. S19. (a, b) XRD characterization of cycled (101)-Zn and (101+002)-Zn metal anode after soaked in 2 M $ZnSO_4$-H_2O for 5 days, (c) Voltage evolution of symmetric Zn half-cell based on (002)-Zn and (101+002)-Zn at current density of 1.0 mA cm^{-2} and areal capacity of 1.0 mAh cm^{-2}.

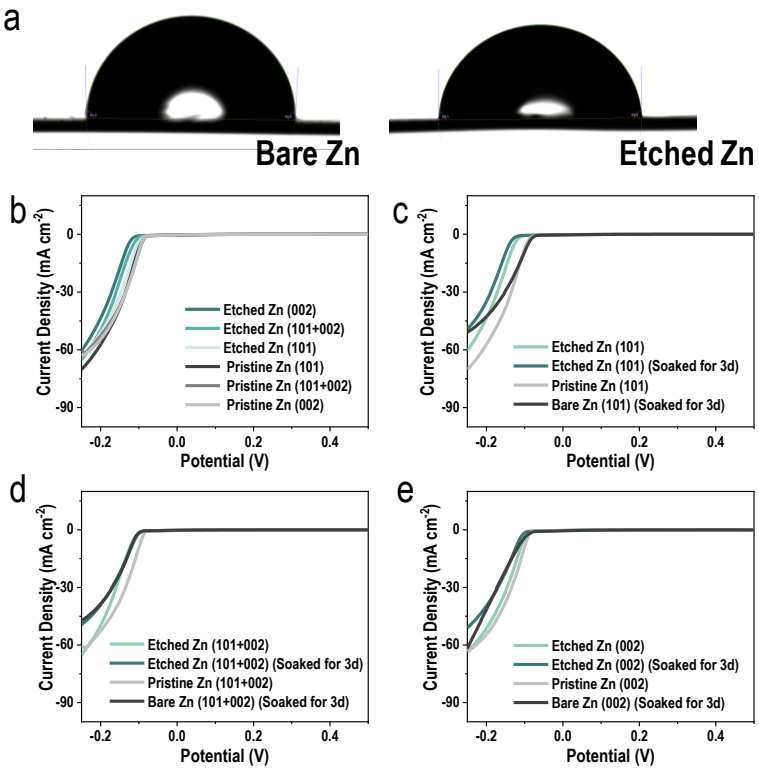

Fig. S20. Mechanism analysis of etched Zn inhibiting side reactions. (a) Contact angle measurement of 2 M $ZnSO_4$ aqueous electrolyte on the surface of bare Zn and etched Zn. (b-e) Linear Scanning Voltammetry (LSV) curves of different Zn metals in the initial state and after three days of rest.

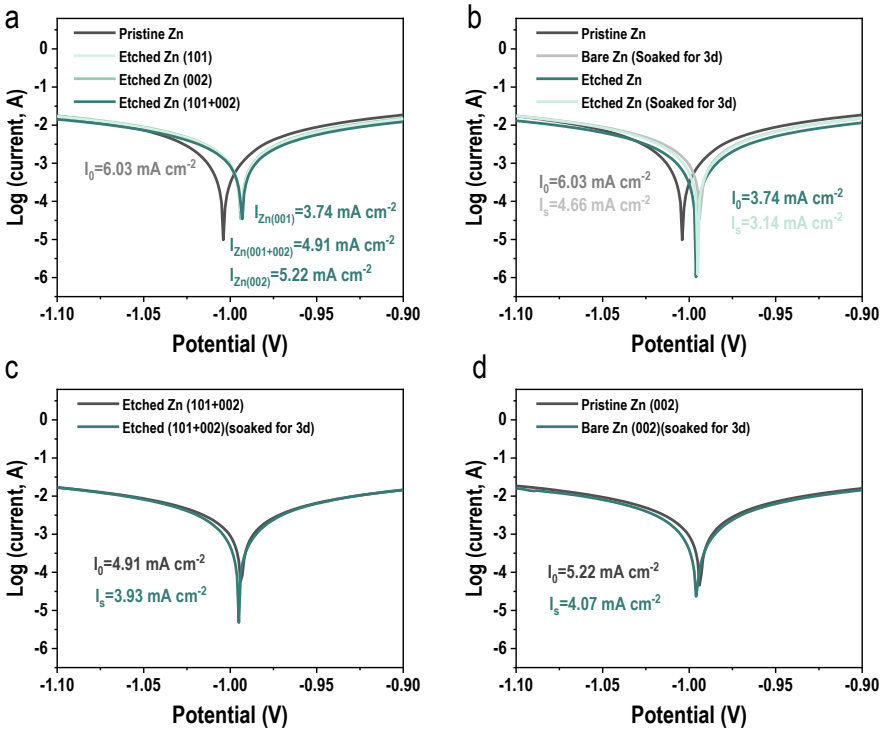

Fig. S21. Linear polarization curves of the bare Zn and etched Zn metals in the initial state and after three days of standing.

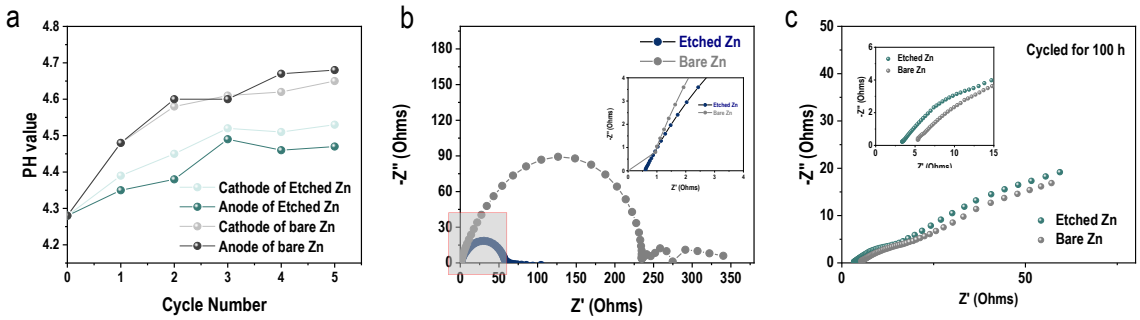

Fig. S22. (a) The in-situ pH tests in the positive and negative regions of batteries with etched Zn and bare Zn as the electrodes during the first five cycles. (b) EIS of bare Zn and etched Zn; (c) EIS of bare Zn and etched Zn after cycling for 100 hours.

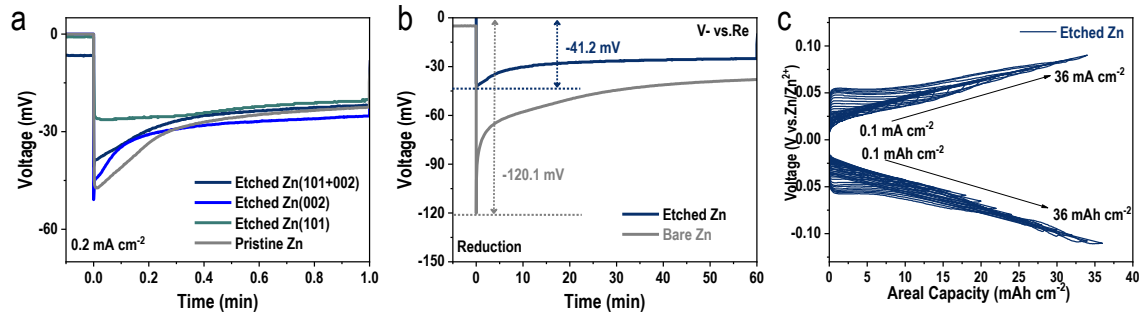

Fig. S23. (a, b) Voltage profiles of bare Zn and etched Zn at a current density of 0.2 and 1.0 mA cm^{-2}; (c) The voltage-capacity curve of Zn//Zn symmetrical cell based on etched Zn under the gradually increasing current density and capacity.

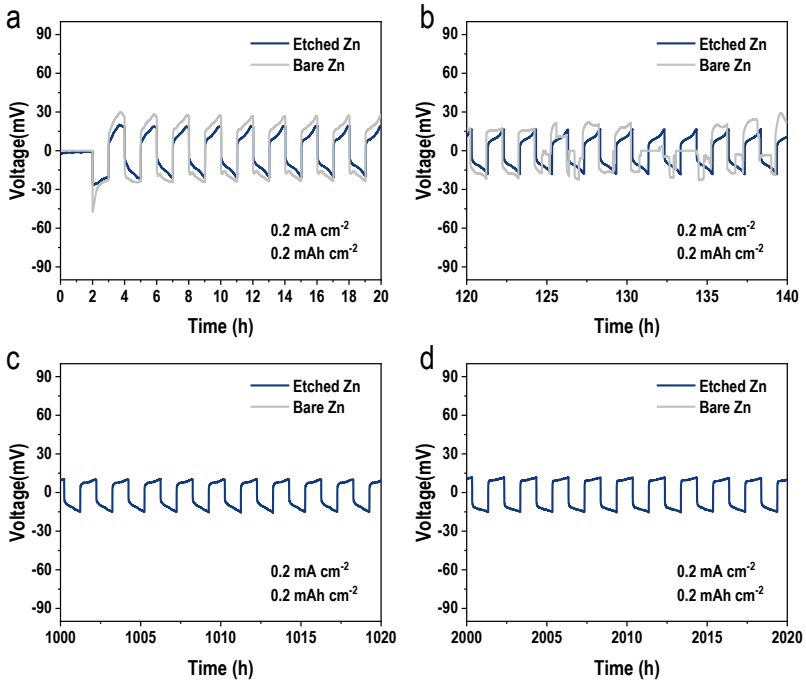

Fig. S24. Voltage evolution of symmetric Zn batteries with bare Zn and etched Zn anodes at current density of 0.2 mA cm^{-2} and areal capacity of 0.2 mAh cm^{-2}.

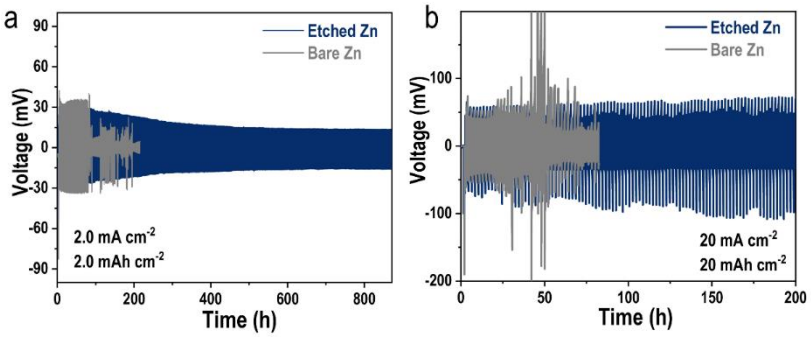

Fig. S25. Symmetric Zn half-cell of bare Zn and etched Zn anodes at different current density and areal capacity.

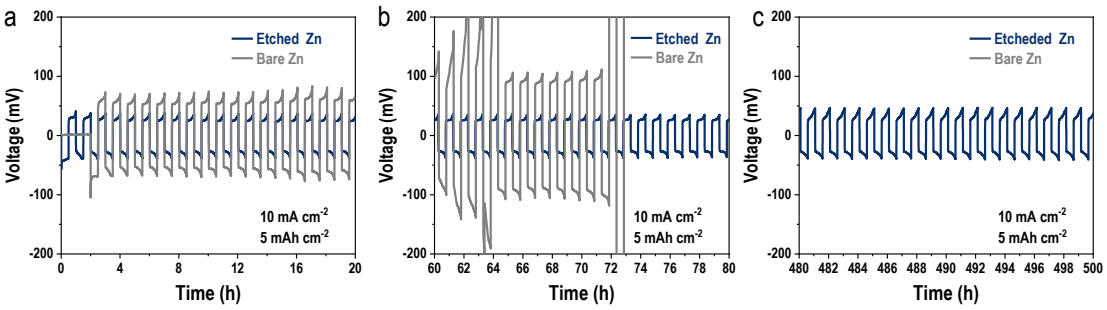

Fig. S26. Voltage evolution of symmetric Zn batteries with bare Zn and etched Zn anodes at current density of 10 mA cm^{-2} and areal capacity of 5 mAh cm^{-2}.

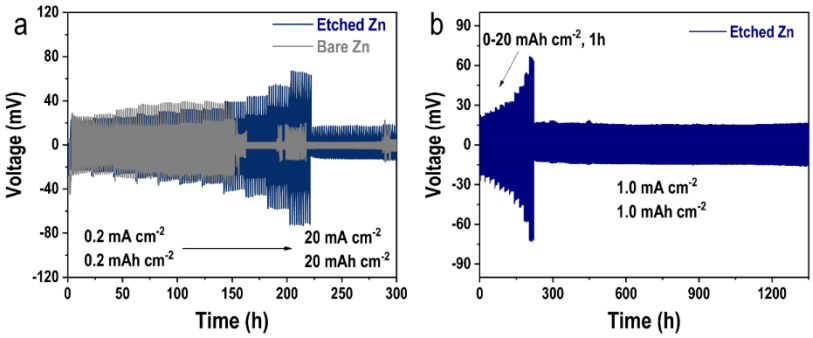

Fig. S27. Rate performances of Symmetrical cells based on the etched Zn and bare Zn metals.

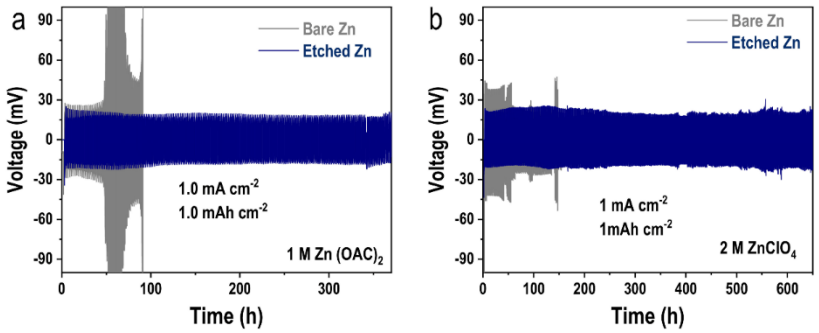

Fig. S28. Voltage evolution of symmetrical Zn half-cell in electrolyte of zinc acetate and zinc perchlorate base on bare Zn and etched Zn at current density of 1.0 mA cm^{-2} and areal capacity of 1.0 mAh cm^{-2}.

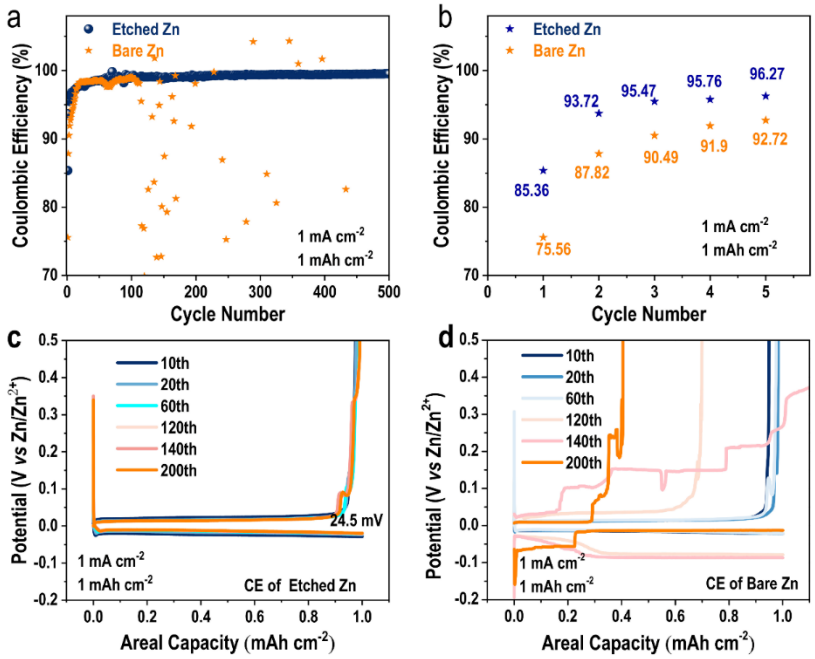

Fig. S29. (a, b) Coulombic efficiency and (c, d) galvanostatic voltage profiles at the different cycles of the asymmetric bare Zn//Cu and etched Zn//Cu cells at 1 mA cm^{-2} with a fixed capacity of 1 mAh cm^{-2}.

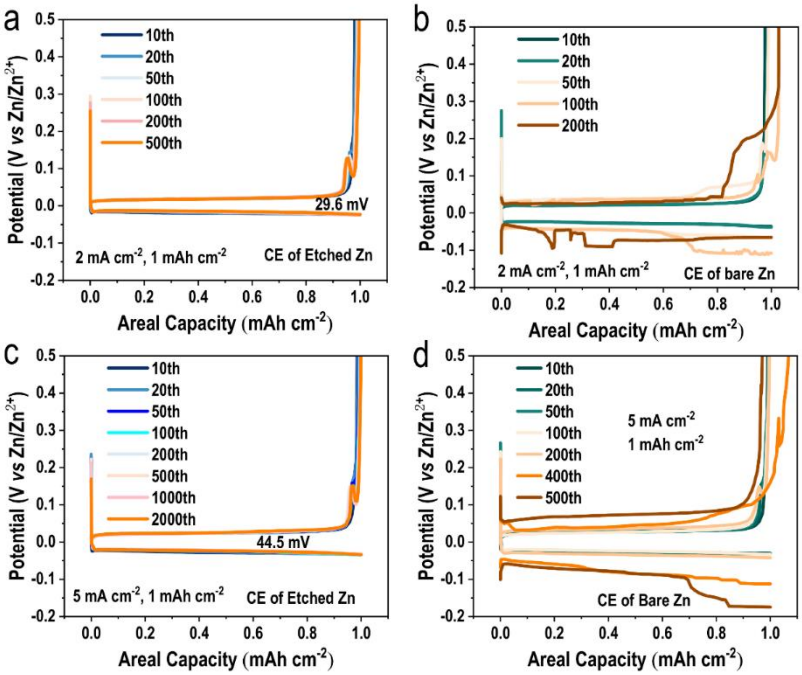

Fig. S30. Galvanostatic voltage profiles at the different cycles of the asymmetric bare Zn//Cu and etched Zn//Cu cells at 2 mA cm^{-2}, 1h and 5 mAh cm^{-2}, 1h. The overvoltage of etched Zn/Cu half-cell was only 29.6 mV and 44.5 mV when the current density at 2 mA cm^{-2} and 5 mA cm^{-2}, respectively.

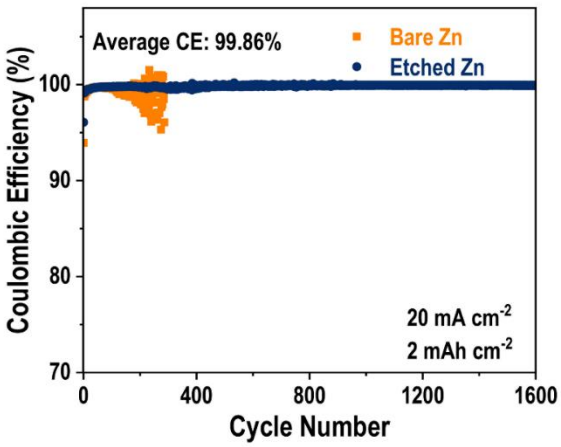

Fig. S31. Coulombic efficiency of the asymmetric bare Zn//Cu and etched Zn//Cu cells at 20 mA cm^{-2} with a fixed capacity of 2 mAh cm^{-2}.

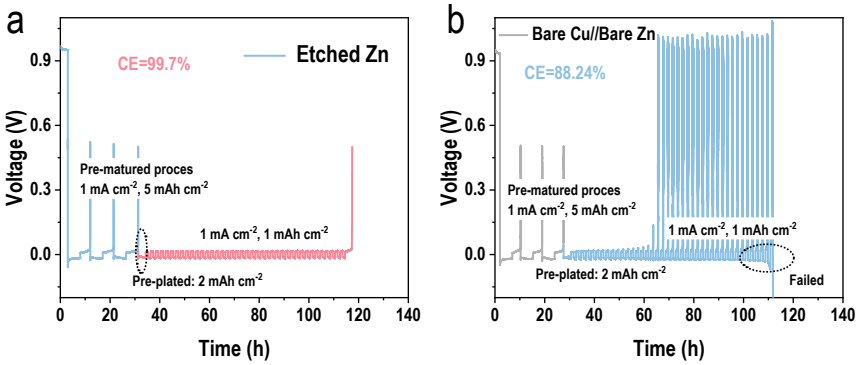

Fig. S32. The time-voltage profiles and corresponding average CE of Zn/Cu cells with three cycles pre-activated mode.

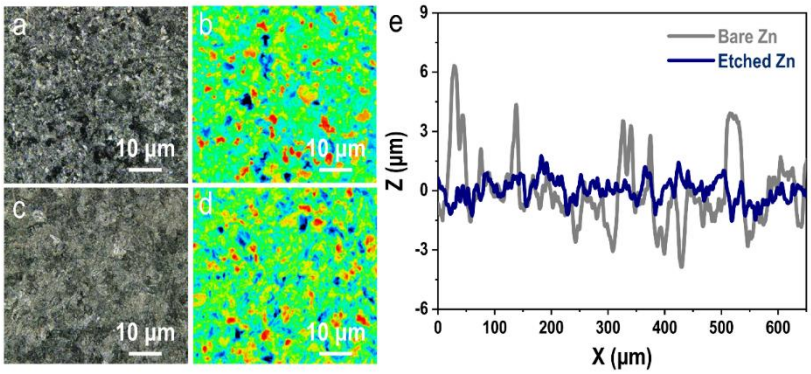

Fig. S33. The Two-dimensional images and the surface height difference of the bare Zn and etched Zn after cycling.

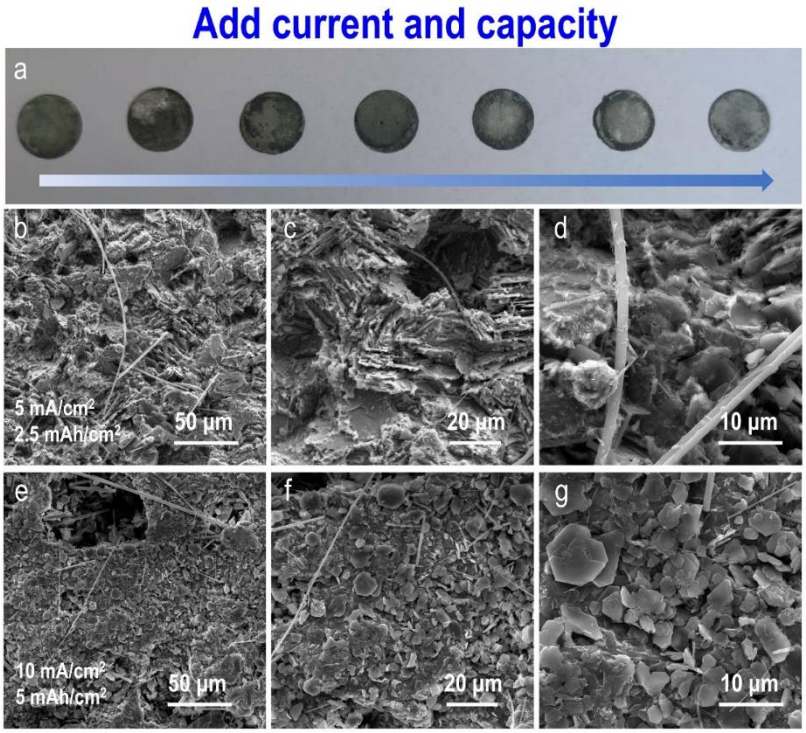

Fig. S34. Images of bare Zn anode collected from symmetrical Zn half-cell. (a) Digital photos of Zn metal anodes at increasing current density. (b-d) SEM images of Zn surface after cycling at 5.0 mA cm^{-2} and 2.5 mAh cm^{-2}. (e-g) SEM images of Zn surface after cycling at 10.0 mA cm^{-2} and 5.0 mAh cm^{-2}.

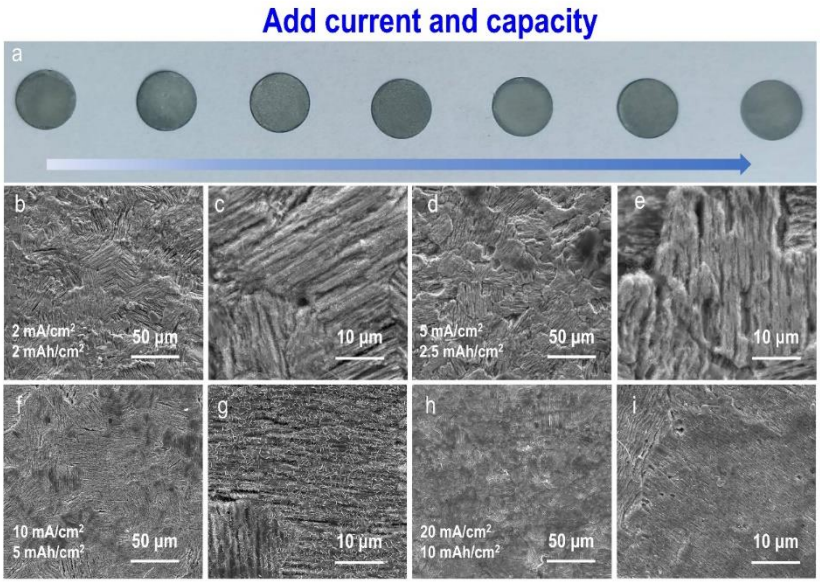

Fig. S35. Images of bare Zn anode collected from symmetrical Zn half-cell. (a) Digital photos of etched Zn anodes at increasing current density. (b-i) SEM images of etched Zn surface after cycling at different current densities and capacities.

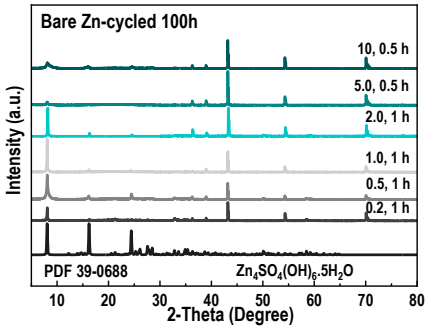

Fig. S36. XRD patterns of cycled bare Zn metals after 100 hours under different current and capacity conditions.

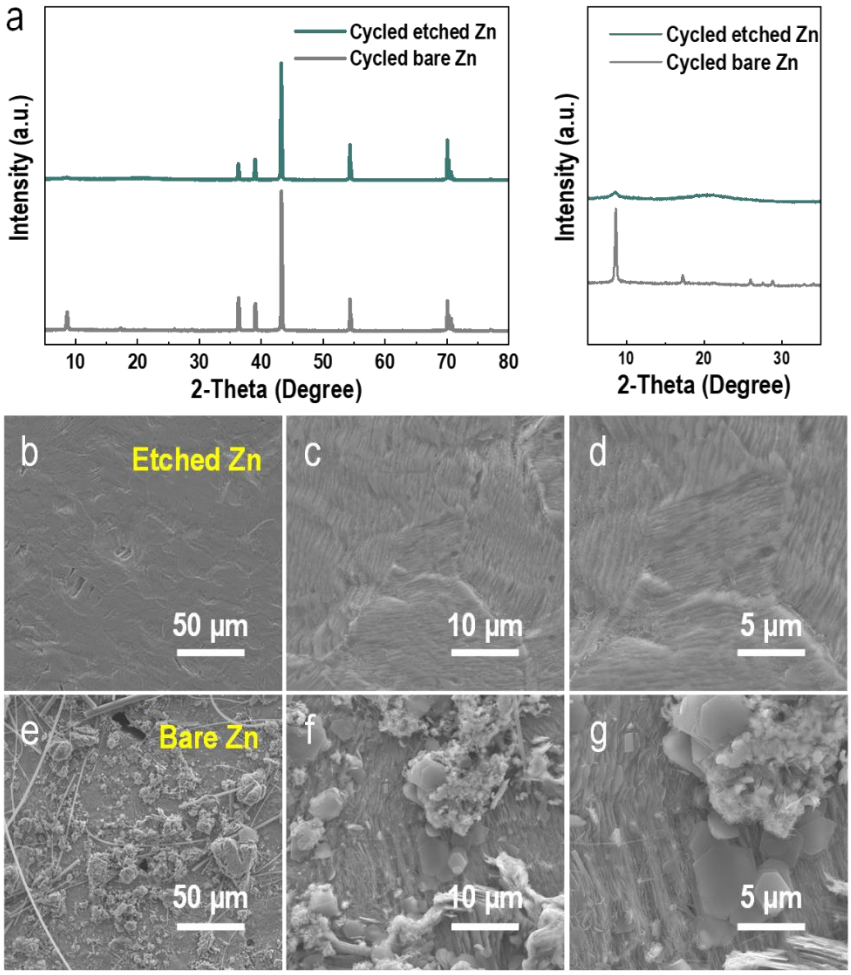

Fig. S37. (a) XRD patterns and SEM images of (b-d) the etched Zn and (e-g) the bare Zn electrodes collected from Zn//Zn symmetrical cells after cycled for 100 hours without 2 hours' pre-rest before testing (under 1 mA/cm^2, 1 mAh/cm^2).

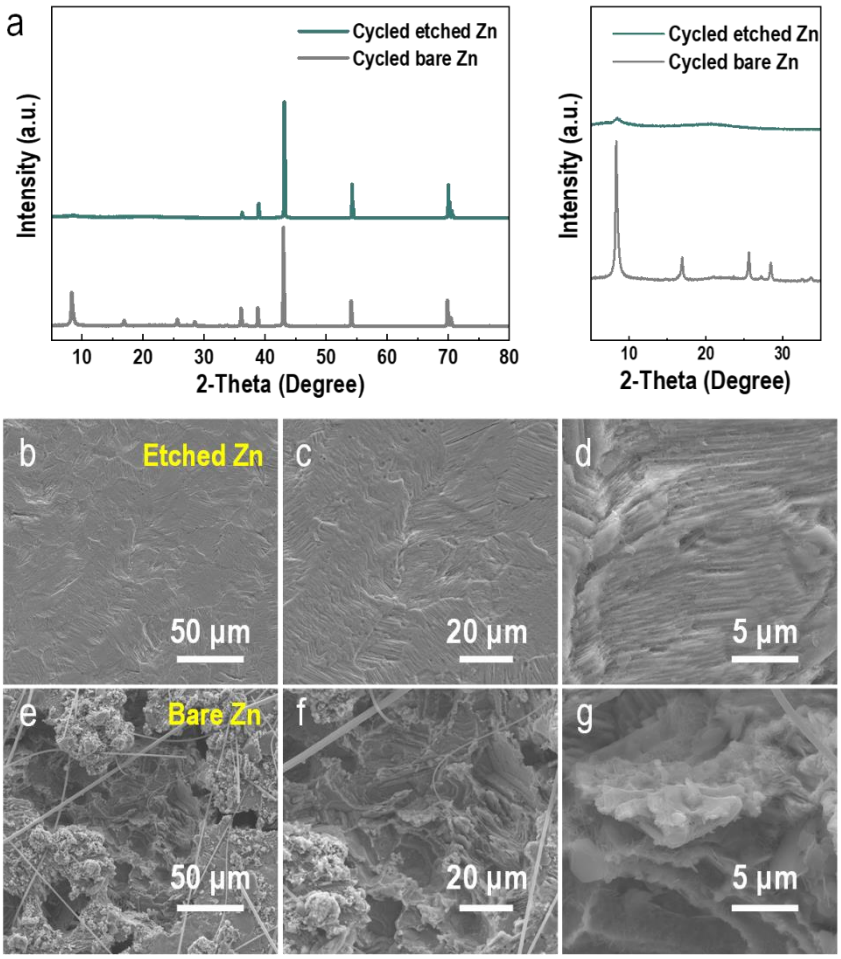

Fig. S38. (a) XRD patterns and SEM images of (b-d) etched Zn and (e-g) bare Zn electrodes collected from Zn//Zn symmetrical cells after cycled for 100 hours under intermittent resting condition of 2 hours after each charge/discharge process (under 1 mA/cm^2, 1 mAh/cm^2).

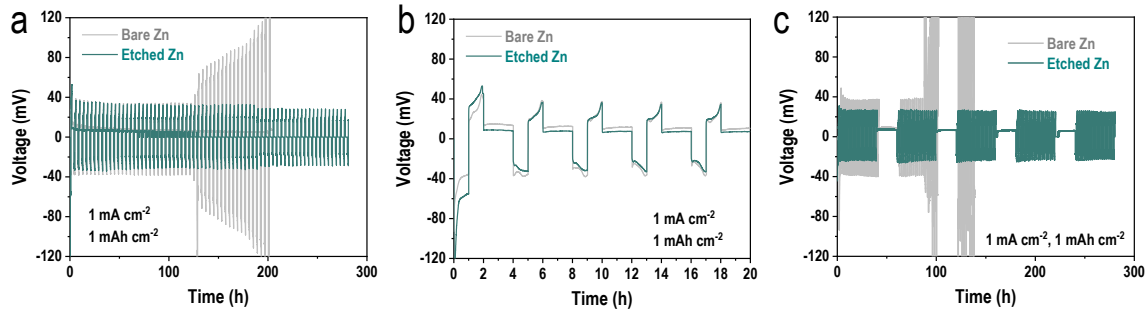

Fig. 39. (a-b) Cycling performance of batteries based on different zinc metals under intermittent resting conditions (2 hours). (c) Cycling performance of symmetrical batteries based on different zinc metals under intermittent resting conditions of 20 hours after each 20 cycles (40 hours).

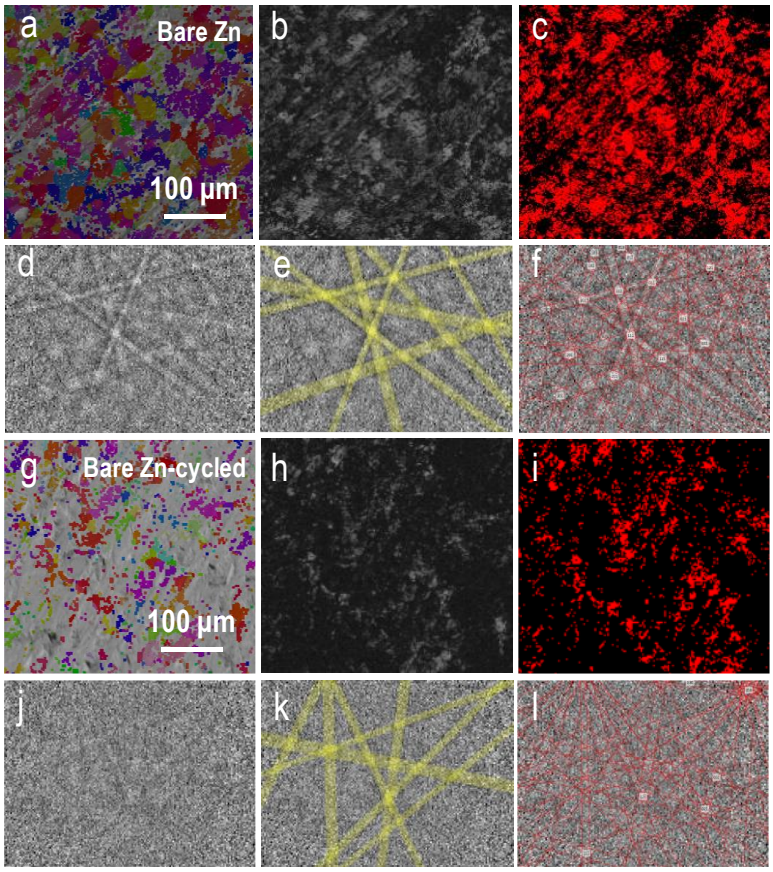

Fig. S40. EBSD results and Kikuchi line of (a-f) pristine Zn and (g-l) bare Zn electrode after deposition.

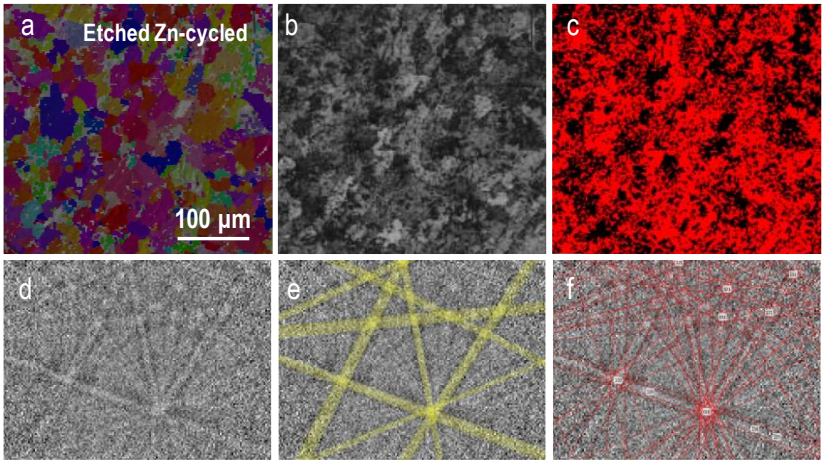

Fig. S41. EBSD results and Kikuchi line of etched Zn metal electrode after deposition.

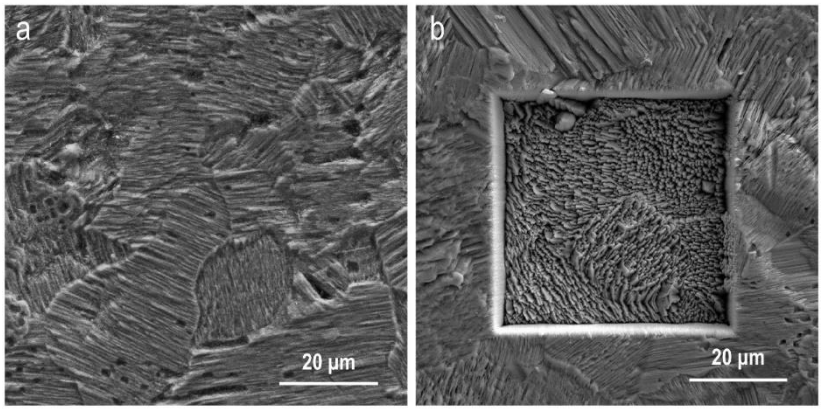

Fig. S42. (a) Vertically aligned and dense electrodeposits of cycled etched Zn. (b) Cross-sectional images produced by focused ion beam (FIB) technique of etched Zn deposits in 2 M $ZnSO_4$-H_2O electrolytes.

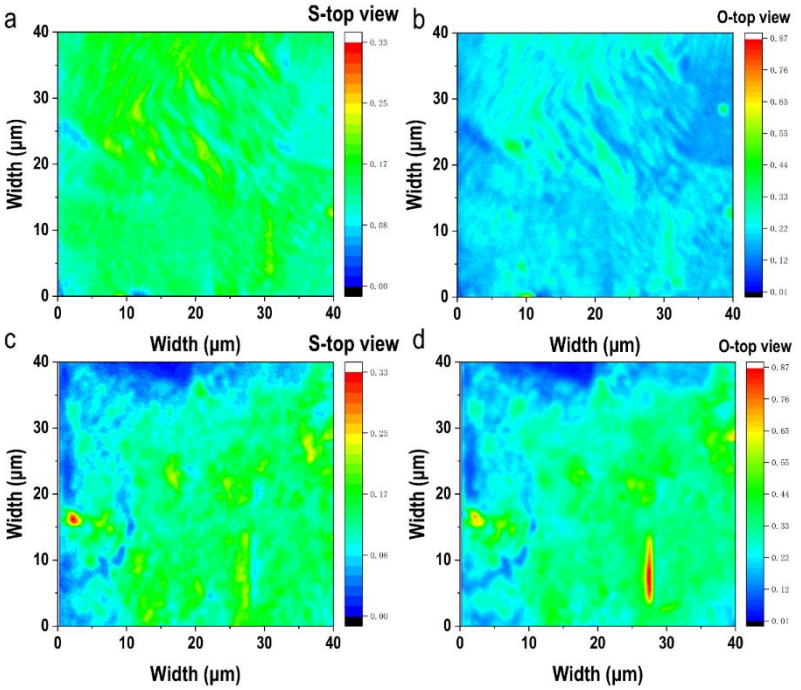

Fig. S43. Two-dimensional distribution of O and S elements on the surface of FIB-cut area. (a, b) Top view of S and O elements on etched Zn anode after cycled; (c, d) Top view of S and O elements on bare Zn anode after cycled.

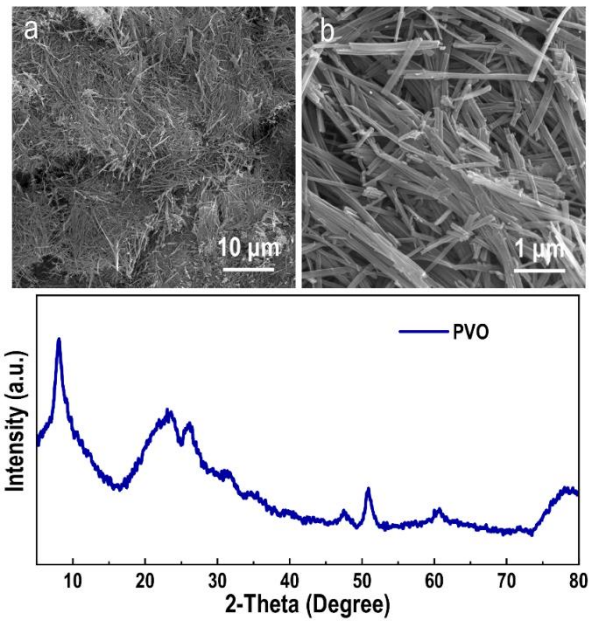

Fig. S44. (a, b) SEM images and (c) XRD Pattern of as-prepared PVO (PANI-V_2O_5).

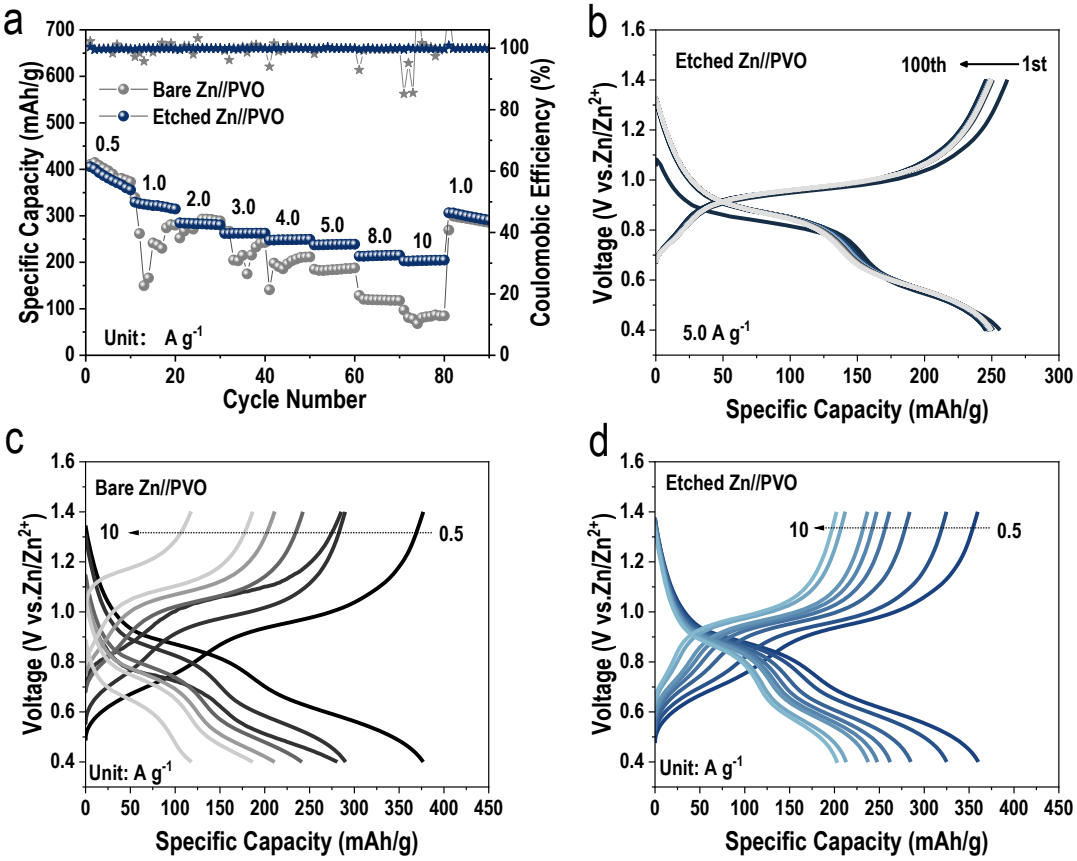

Fig. S45. (a) The rates performances of PVO//Zn half-cell based on bare Zn and etched Zn; (b) The charge-discharge curves of PVO//Zn half-cell; (c, d) Voltage profile of Zn//PVO batteries based on different electrodes (bare Zn and etched Zn) at different current densities.

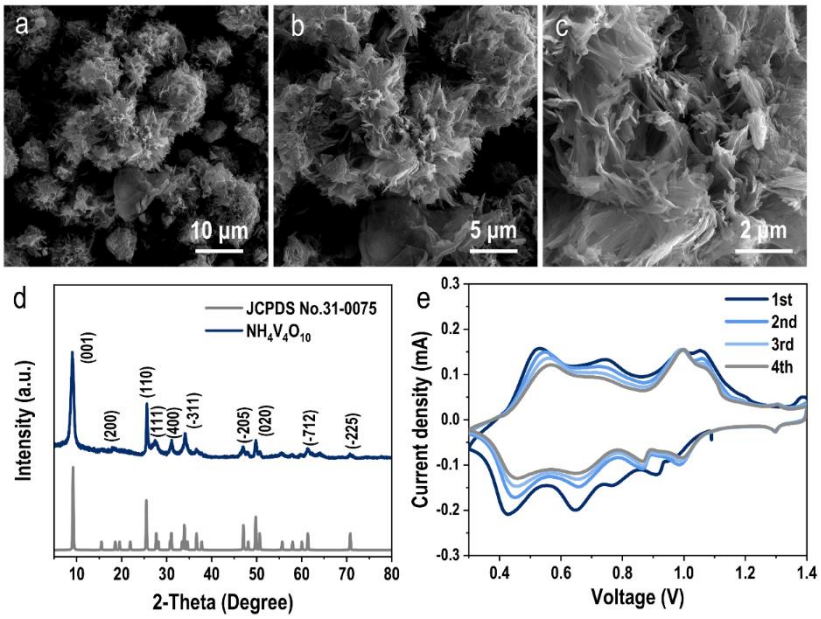

Fig. S46. (a, b, c) SEM images, (d) XRD Pattern and the CV of as-prepared $NH_4V_4O_{10}$.

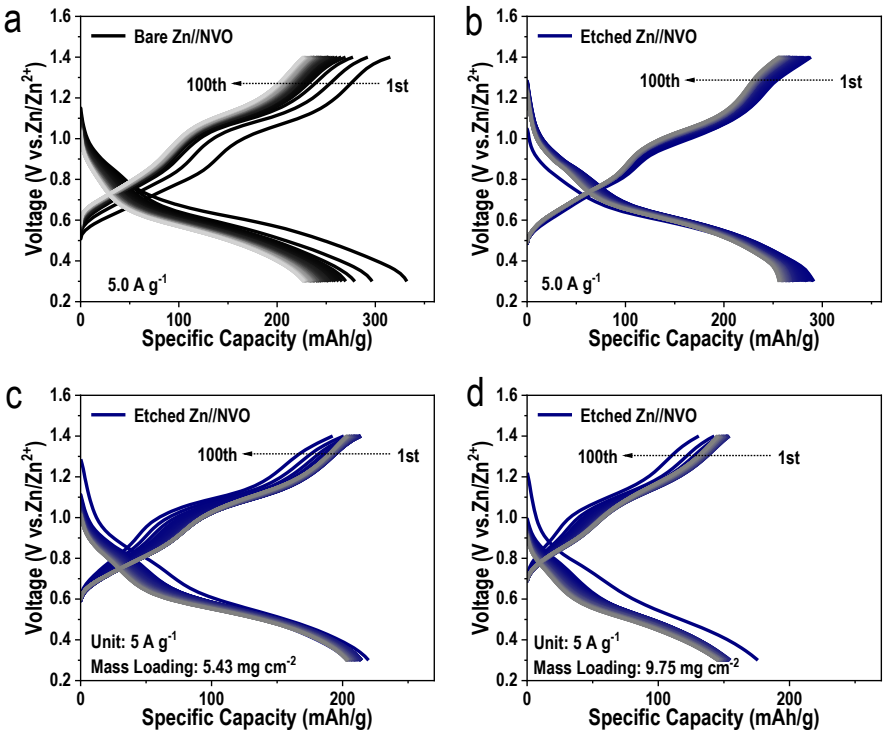

Fig. S47. (a, b) Voltage profile of Zn//NVO batteries at current density of 5 A g^{-1}; (c, d) Voltage profile of Zn//NVO batteries with different mass loading of NVO cathode.

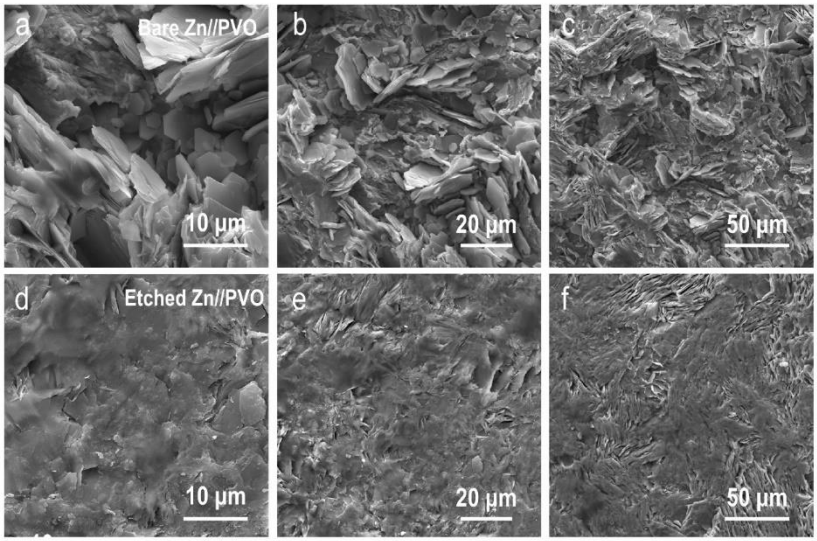

Fig. S48. The SEM images of (a, b, c) bare Zn and (d, e, f) etched Zn metals collected from the cycled half-cells (PVO//Zn half-cells).

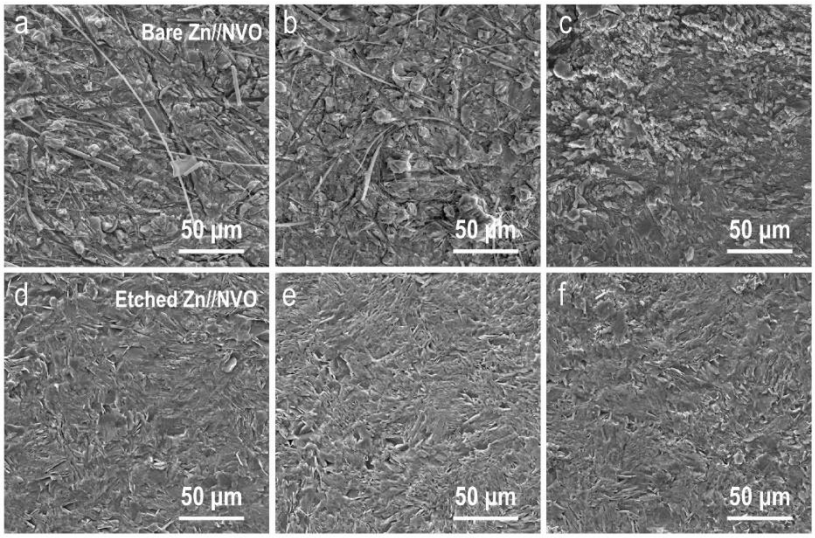

Fig. S49. The SEM images of (a, b, c) bare Zn and (d, e, f) etched Zn metals collected from the cycled half-cells (NVO//Zn half-cells).

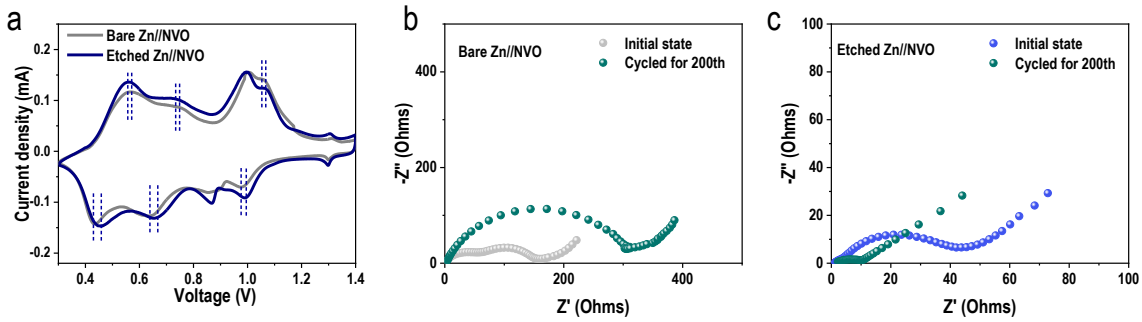

Fig. S50. (a) The voltage gap of the redox peak of the NVO//Zn based on etched Zn and bare Zn; (b, c) EIS results of Zn//NVO cells based on different electrodes (bare Zn, etched Zn) after 200 cycles.

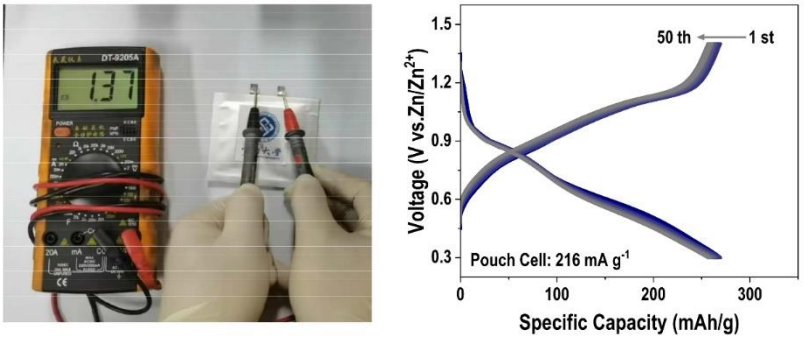

Fig. S51. The open circuit voltage and the galvanostatic charge/discharge profiles of pouch-cell.

Table S1. The grain indexing rate and phase percentage of the pristine Zn, cycled bare Zn and cycled etched Zn.

Samples	Phase name	Percentage of phase (%)	Phase counting	Average band contrast	Minimum band contrast	Maximum band contrast
Bare Zn	Zinc	**15.67**	3072	72.48	17.00	172.00
	Zero resolution	84.33	16528	30.81	0.00	153.00
Bare Zn-cycled	Zinc	**8.29**	4503	63.57	13.00	161.00
	Zero resolution	91.71	49786	28.55	0.00	186.0
Etched Zn-cycled	Zinc	**56.97**	16080	86.85	22.00	186.00
	Zero resolution	43.03	12144	45.30	0.00	211.0